Simple and Convenient Design of a Spectroelectrochemical Cell for *In Situ* XANES Measurements of Adsorbed Species in Transmission Mode

Guang Shan Xuan, Sukman Jang, Gwanghoon Kwag,[†] and Sunghyun Kim[*]

Department of Chemistry and BioMolecular Informatics Center, Konkuk University, Seoul 143-701, Korea
[*]E-mail: skim100@konkuk.ac.kr
[†]Kumho Chemical Laboratories, Kumho Petrochemical Co., Daejeon 305-600, Korea
Received March 4, 2005

X-ray absorption fine structure (XAFS) spectroscopy has now become a versatile tool for the structural analysis.[1-3] Not requiring a long-range order, XAFS has been applied to various fields of science where crystalline samples cannot be prepared. Electrochemistry also found XAFS very useful in elucidating electrochemical interfaces modified with foreign metals and molecular species. Since these interfaces often display very different electrochemical properties from those of unmodified surfaces, thus playing a key role in many electrochemical processes, it is crucial to characterize them at an atomic or molecular level. Among many surface sensitive techniques, XAFS based on synchrotron radiation is peculiar in that vacuum is not required and is directly applicable to the electrochemical systems.[4]

X-ray absorption near edge structure (XANES) as a part of XAFS represents fine structures arising from electronic transitions of core electrons to the bound states within ca. 30 eV above absorption edge. XANES has been known to provide both electronic and structural information. Different fine structures are resulted when an absorbing atom undergoes redox reactions or the symmetry around it changes.[5] Therefore, the close inspection of XANES provides with valuable information such as oxidation state of an absorbing atom and geometrical environment.

Designing *in situ* cells for electrochemical measurements has some peculiarities comparing to other *in situ* experiments. Unlike with the UV/visible light, *in situ* studies of electrode surfaces with X-ray are generally complicated due to the spurious absorption of electrolyte especially at low or moderately high X-ray energies.[6] The situation becomes even worse when the number of absorbing atoms is small and the cell components such as cell windows and electrode materials along the beam path are present. Thus it would require an enormous amount of time to collect analyzable data. With this reason, *in situ* XAFS measurements for the first transition metals in transmission mode are very difficult.

Nonetheless, many attempts have been made to simultaneously collect both electrochemical and spectroscopic data. Some electrochemical systems are intrinsically suitable for the transmission mode measurements. Among them are battery materials and metal oxide systems as demonstrated by McBreen[7] and Melendres,[8] where the metal portion is quite high and the whole electrode material is electrochemically active so that a spectrum of high S/N ratio can be obtained. If the species of interest is soluble in electrolyte, a thin-layer cell devised by Heineman *et al.*[9,10] can be used, where the bulk electrolysis by the reticulated vitreous carbon is performed.

The situation becomes quite different when it comes to the study of adsorbed species as the electrode surface accommodates only limited amount of species per unit area. Abruña *et al.*[11] electropolymerized metal complexes and used grazing incidence geometry to enhance the signal from the surface. Multi-layer coverage is needed to acquire good quality data and warrant that all the adsorbed molecules are electrochemically active must be secured. The best way is thus to collect XAFS for the monolayer. Several attempts have been made to increase the adsorption amount while maintaining the monolayer coverage. Kim *et al.*[12-14] used high-area carbon powder (surface area > 1000 m²) as a supporting material to accommodate as much compound as possible. This method has been successfully applied to metalloporphyrins and phthalocyanines to monitor the structural changes upon oxidation state change. However, a long sample preparation time and complications in an experimental setup have been a drawback. Another weak point is that only fluorescence mode measurements are possible.

In an effort to circumvent difficulties mentioned above, here we report the construction of an *in situ* cell that can be used in transmission mode and tested its performance with cobalt sepulchrate and iron hydrous oxide formed on electrode surfaces. Reliable XANES spectra could be obtained with a reasonable amount of time.

Experimental Section

A schematic diagram of the *in situ* cell is shown in Figure 1. The working electrode made of a carbon sheet (Garam Carbon, Korea) is sandwiched between two filter papers soaked with electrolyte. The carbon sheet (0.4 mm thick) was peeled off by adhesive tape to increase the surface area to incorporate as much compound as possible. The peeled surface was first treated with 1 M HCl to provide the surface with hydrophilicity. A thin Kapton tape was put on the outer surfaces of two filter papers to prevent electrolyte from
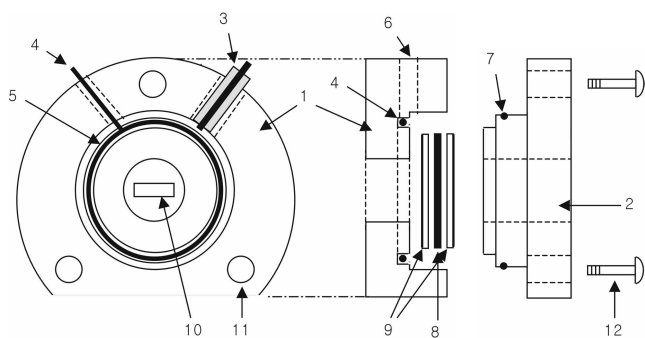
Figure 1. Schmatic diagram of the *in situ* cell. 1: Teflon cell body 1, 2: Teflon cell body 2, 3: reference electrode. 4: Pt counter electrode. 5: groove for counter electrode, 6: hole for reference electrode and electrolyte injection, 7: O-ring. 8: carbon sheet working electrode. 9: filter paper with Kapton tape. 10: X-ray beam path, 11: screw hole, 13: screw.

leaking. In this way, filter papers also serve as cell windows. The Pt counter electrode was placed in a circular hole formed around the working electrode in order to avoid blocking X-ray beam path. The reference electrode (Ag | AgCl | 3.5 M KCl) was placed onto the cell body. Electrolyte solution was injected through the hole inside the cell. In this thin layer type configuration, the reduction of X-ray beam intensity due to the scattering effect of electrolyte could be minimized, with electrochemistry still possible.

XANES spectra were acquired at Electrochemistry beam-line of Pohang Light Source (PLS) operating at energy of 2.50 GeV with a ring current of 130-190 mA. This beamline does not use any insertion devices to increase beam intensity but only bending magnets. The beam was monochromatized by a Si(111) double crystal with an exit slit adjusted to 1×5 mm^2. The monochromator was detuned by 25% to reject higher harmonics. The energy calibration was done with a corresponding metal foils. The first inflection point was set as E_0 and used to calibrate all data.

Cobalt(III) sepulchrate trichloride (1,3,6,8,10,13,16,19-octaazabicyclo[6,6,6]eicosanecobalt trichloride, CoSep, Aldrich, Milwaukee, MW = 451.7) (Figure 2) was chosen as a model system to test the performance of this *in situ* cell. CoSep undergoes one-electron transfer process and has been
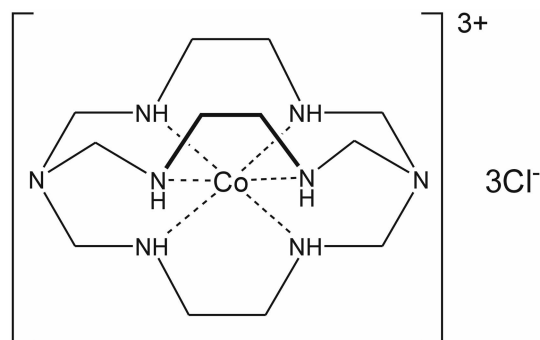

Figure 2. The structure of cobalt sepulchrate trichloride (1,3,6,8,10,13,16,19-octaazabicyclo[6,6,6] eicosane cobalt trichloride).
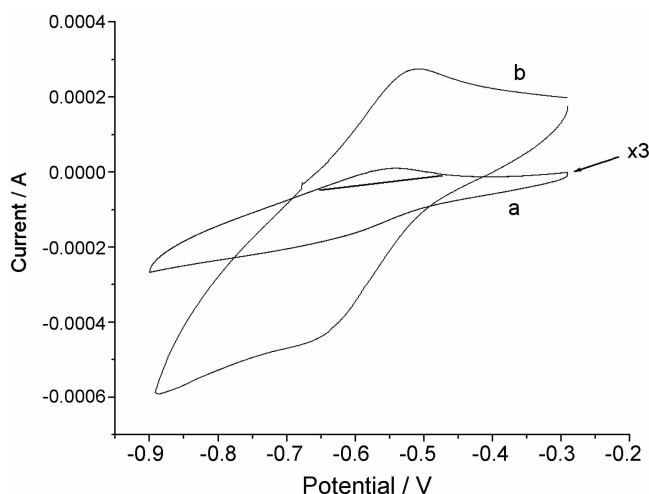

Figure 3. Cyclic voltammograms of adsorbed CoSep (curve a) and 1.0 mM CoSep (curve b) with scan rates at 2 and 50 mV·s^{-1}, respectively.

used as a redox mediator.[15] A carbon sheet was soaked in 1.0 mM CoSep solution for 20 min to ensure the adsorption. After carefully washing with electrolyte (0.10 M KCl), the electrode was set in the cell.

Iron hydrous oxide films were prepared by passing 1 mA cathodic current for 5 min from 0.05 M Fe(NO$_3$)$_3$ solution. Nitrate reduction near the working electrode raises pH which in turn makes iron hydrous oxide film formed on the surface.[16] After washing the film with water, the electrode was immediately put into the *in situ* cell and examined by cyclic voltammetry in 1.0 M KOH solution.

Results and Discussion

The *in situ* cell has been characterized by cyclic voltammetry. Curve a in Figure 3 is the cyclic voltammogram of CoSep monolayer obtained at 2 mV·s^{-1}. The peak separation of *ca.* 80 mV at this low scan rate indicates that the solution resistance is very high due to the thin layer geometry. Curve b is obtained for the 1.0 mM CoSep dissolved in solution. E_p of 130 mV at 50 mV·s^{-1} is indicative of a quasi-reversible nature of CoSep. At lower scan rate, E_p becomes smaller. Note that adsorbed CoSep can also contribute to the voltammogram in this case.

The adsorbed amount was calculated by integrating area under the voltammetric peak. It was 3×10^{-9} mol per apparent electrode area. This value for a monolayer is quite high compared to that at a smooth surface. The monolayer coverage on the smooth surface is between 10^{-10} and 10^{-11} mol·cm^{-2} depending on the molecular size. For example, cobalt tetrasulfonated phthalocyanine has a coverage of 3×10^{-11} mol·cm^{-2} at highly oriented pyrolytic graphite. The high loading of the molecule is due to the roughened electrode surface as we intended. Since the X-ray beam dimension is 8.0 mm $\times$ 1.0 mm, the number of exposed molecules is 1.4×10^{14}.
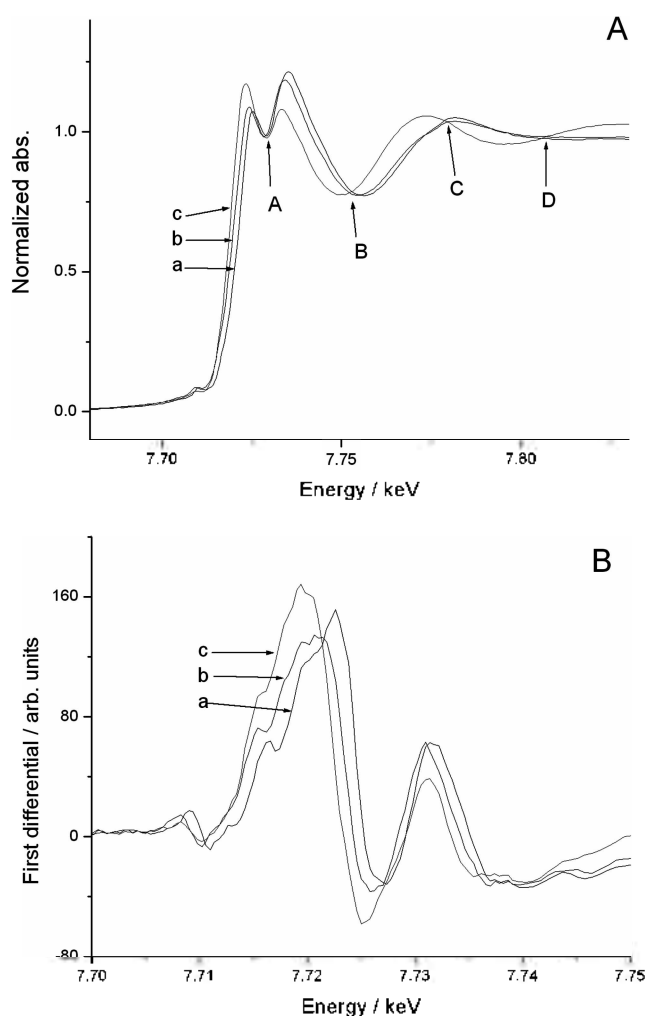
Figure 4 shows a series of normalized (Panel A) and first

Figure 4. Normalized (Panel A) and first differential (Panel B) XANES spectra for CoSep at different polizations. Curves a-c represent XANES. respectively. for fully oxidized. partially reduced. and fully reduced CoSep.

Figure 5. A series of XANES spectra for iron hydrous oxide. Curves a-d represent XANES. respectively. for fully oxidized (FeOOH), two partially reduced, and fully reduced (Fe(OH)₂) iron hydrous oxides.

differential (Panel B) XANES spectra under different conditions. Identical spectra are obtained for the pure CoSep, adsorbed CoSep without potential applied, and adsorbed CoSep polarized at −0.3 V (curve a) at which potential cobalt remains at +3 state. This means that the molecular structure of CoSep is not altered upon adsorption or potential influence as long as Co oxidation state is maintained constant. The pre-edge peak found at 7710.2 eV has been known as a dipole-forbidden but quadrupole-allowed $1s \rightarrow 3d$ transition.[12] This transition is resulted from orbital mixing between metallic d- and ligand p-characters. The position and intensity of this peak indicate the oxidation state of an absorbing atom and site symmetry.

Curves b and c were obtained by polarizing the electrode at which adsorbed Co(III)Sep was partially and fully reduced to Co(II)Sep. The reduction gives rise to the overall spectral shift to a lower energy. The inflection point for the Co K-edge rise was shifted by 3.2 eV to lower energy from 7722.6 eV to 7719.4 eV upon full reduction from Co(III) to Co(II). The partial reduction gives a smaller shift. At least
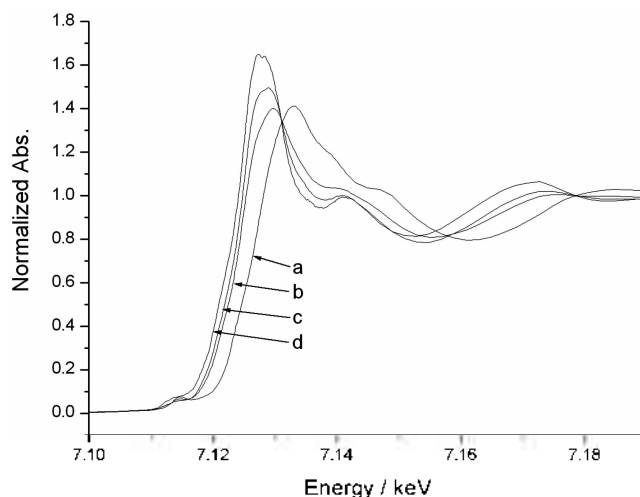
four isosbestic points appeared at A, B, C, and D. This is indicative of the presence of only two cobalt species, Co(II)Sep and Co(III)Sep.

The pre-edge peak shift was also observed. According to the Kunzl,[17] the energy positions (either pre-edge or main absorption edge) are linearly related to the formal valency of the element. The pre-edge position was changed from 7709.2 eV to 7708.1 eV by 1.1 eV. The negative shift in the transition energy with valency is due to the decrease of the attractive potential of a nucleus on the 1s electron. 1 eV shift in pre-edge position is approximately equivalent to the valency change of 1. Also noteworthy is the pre-edge peak intensity in that it reflects the site symmetry around an absorbing atom. Lower symmetry gives rise to higher intensity. A close inspection tells that the peak intensity decreased upon reduction. This explains that octahedral geometry around the cobalt atom becomes a little more symmetrical when reduced.

As a further evaluation of the cell, another *in situ* measurement has been performed in which structural changes of iron hydrous oxide film formed on an electrode surface have been studied as a function of oxidation state. The produced film has a loose structure containing water molecules in it but undergoes a reversible electrochemical reaction. In analogy with Ni and Co hydrous oxides, the reaction may be written as follows in alkaline solutions.[16,18]

$$FeOOH + H_2O + e \leftrightarrow Fe(OH)_2 + OH$$
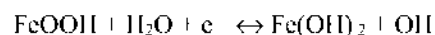
Polarization at potentials where FeOOH and Fe(OH)₂ are formed gives rise to a series of XANES spectra with energy shift as expected (Fig. 5). Both edge and pre-edge shift demonstrate that this *in situ* method is quite reliable. Multi-scanning gave the exactly same results, indicating that all of the iron species change its oxidation state. This is contrary to the cobalt oxide case in which electrochemically unseen cobalt compound exists.[18]

Conclusions

A simple and convenient *in situ* electrochemical cell for XAFS measurements has been made. Good quality of XANES spectra could be easily collected with this cell for the adsorbed organometallic species in transmission mode; otherwise a long sample preparation and complex measuring process is required. XANES changes induced by the potential excursion could be seen in an ordinary synchrotron facility. The results demonstrate that this cell can find applications in many organometallic compounds where the structural and electronic aspects as a function of metal oxidation state are of interest.

References

1. Penner-Hahn. J. *Coord. Chem. Rev.* **1999**, *190-192*, 1101.
2. *X-ray Absorption: Principles, Applications, Techniques of EXAFS, SEXAFS, and XANES*, Koningsberger. D. C., Prins, R., Eds.; Wiley: New York, 1998.
3. Teo, B. K. *EXAFS: Basic Principles and Data Analysis*, Springer: New York, 1986.
4. Park. Y. J.; Hong. Y. S.; Wu. X.; Kim. M. G.; Ryu. K. G.; Chang. S. H. *Bull. Korean Chem. Soc.* **2004**, *25*, 511.
5. Kwag. G.; Park. E.; Kim. S. *Bull. Korean Chem. Soc.* **2004**, *25*, 298.
6. Sharpe, L. R.; Heineman, W. R.; Elder. R. C. *Chem. Rev.* **1990**, *90*, 705.
7. McBreen. J.; O'Grady, W. E.; Tourillon. G.; Dartyge. E.; Fontaine. A.; Pandya. K. I. *J. Phys. Chem.* **1989**, *93*, 6308.
8. Melendres. C. A.; Mansour. A. N. *Electrochim. Acta* **1998**, *43*, 631.
9. Smith. D. A.; Elder. R. C.; Heineman. W. R. *Anal. Chem.* **1985**, 2361.
10. Smith. D. A.; Heeg. M. J.; Heineman. W. R.; Elder. R. C. *J. Am. Chem. Soc.* **1984**, *100*, 3053.
11. Albarelli. M. J.; White. J. H.; Bommarito. G. M.; McMillan. M.; Abruna. H. D. *J. Electroanal. Chem.* **1988**, *248*, 77.
12. Kim. S.; Bae. I. T.; Sandifer. M.; Ross, P. N.; Carr. R.; Woicik, J.; Antonio. M. R.; Scherson. D. A. *J. Am. Chem. Soc.* **1991**, *113*, 9063.
13. Ha. S. Y.; Park. J.; Ohta. T.; Kwag. G.; Kim. S. *Electrochem. Solid State Lett.* **1999**, *2*, 461.
14. Kim. S.; Ohta. T.; Kwag. G. *Bull. Korean Chem. Soc.* **2000**, *21*, 588.
15. Reipa. V.; Mayhew. M. P.; Vilker, V. L. *Proc. Natl. Acad. Sci. USA* **1997**, *94*, 13554.
16. Kim. S.; Tryk. D. A.; Antonio. M. R.; Carr. R.; Scherson. D. A. *J. Phys. Chem.* **1994**, *98*, 10269.
17. Kunzl. V. *Collect. Trav. Chim. Techoselovaquie* **1932**, *4*, 213.
18. Totir. D.; Mo. Y.; Kim. S.; Antonio, M. R.; Scherson, D. A. *J. Electrochem. Soc.* **2000**, *147*, 4594.